Characterization of Bi_2Te_3 and Bi_2Se_3 topological insulators grown by MBE on (001) GaAs substrates

Xinyu Liu[a)]
Department of Physics, University of Notre Dame, Notre Dame, Indiana 46556

David J. Smith
Department of Physics, Arizona State University, Tempe, Arizona 85287

Helin Cao and Yong P. Chen
Department of Physics, Purdue University, West Lafayette, Indiana 47907

Jin Fan
Department of Physics, Arizona State University, Tempe, Arizona 85287 and Center for Photonics Innovation, Arizona State University, Tempe, Arizona 85287

Yong-Hang Zhang
Center for Photonics Innovation, Arizona State University, Tempe, Arizona 85287 and School of Electrical, Computer and Energy Engineering, Arizona State University, Tempe, Arizona 85287

Richard E. Pimpinella, Malgorzata Dobrowolska, and Jacek K. Furdyna
Department of Physics, University of Notre Dame, Notre Dame, Indiana 46556

(Received 16 September 2011; accepted 20 November 2011; published 9 December 2011)

Films of pseudohexagonal Bi_2Te_3, Bi_2Se_3 and their alloys were successfully grown by molecular beam epitaxy on GaAs (001) substrates. The growth mechanism and structural properties of these films were investigated by reflection high-energy electron diffraction, atomic force microscopy, x-ray diffraction (XRD), high-resolution transmission electron microscopy, and Raman spectroscopy and mapping. The results indicate that the epitaxial films are highly uniform and are of high crystalline quality. © *2012 American Vacuum Society*. [DOI: 10.1116/1.3668082]

I. INTRODUCTION

The recent discovery of quantum spin Hall effect (QSHE) in two-dimensional (2D) HgTe quantum wells[1] has stimulated an intensive search for three-dimensional (3D) topological insulators (TI), a new state of matter with topologically nontrivial band structures originating from strong spin-orbit coupling (SOC).[2,3] Angle-resolved photoelectron spectroscopy (ARPES) measurements have confirmed the 3D TI behavior in a number of materials—$Bi_{1-x}Sb_x$,[4] Bi_2Se_3,[5] Bi_2Te_3,[6] and Sb_2Te_3,[7] —all of which show an insulating energy gap in the bulk and gapless surface state(s) with Diraclike linear band dispersion. Theoretical models predict that these TI surface states are "topologically protected" and are characterized by extremely high mobilities and spin-locked transport,[3] thus opening up interesting opportunities for applications in spintronics.[8]

In order to study fundamental TI properties, high quality TI films need to be interfaced with superconductors, ferromagnets or other materials. For this reason, molecular beam epitaxy (MBE) is especially attractive because of its capability for growing multilayer heterostructures under highly controlled conditions, so that defect formation is minimized during growth. Most efforts to fabricate TI films by MBE have so far been carried out using substrates with a hexagonal or three-fold symmetric surface structure, such as Si (111),[9,10] sapphire[11] or $SrTiO_3$ (111) (Ref. 12) substrates, with some limited work done on GaAs (111) substrates.[13] Because the representative spintronic materials, such as GaMnAs, are usually grown on GaAs (001) substrates,[14] and Fe films of very high crystalline perfection can also be grown on GaAs (001) and (110) surfaces,[15] in this work we have extended MBE growth of Bi_2Te_3, Bi_2Se_3 and their alloys to deposition on the *symmetrically-mismatched* GaAs (001) substrates. Such novel growth mode may enable one to combine almost any pair of layered materials together; thus allowing us to produce a variety of new high quality semiconductor heterostructures. Our work reveals unique layer-by-layer growth of these materials in a pseudohexagonal layered structure—a crystalline structure that involves sequences of five atomic layers [quintuple layers (QLs), e.g., Te(1)-Bi-Te(2)-Bi-Te(1) or Se(1)-Bi-Se(2)-Bi-Se(1)], with each atomic Te/Se or Bi layer within the QL forming a 2D hexagonal lattice perpendicular to the *c*-axis. Our observations suggest a powerful new possibility for incorporating the highly attractive properties of TI materials with traditional electronic materials that are more compatible with the cubic structure, to construct novel multifunctional device configurations.

II. FABRICATION AND EXPERIMENTAL DETAILS

TI films, including Bi_2Te_3, Bi_2Se_3 and their ternary alloys, were grown using a dual-chamber Riber 32 solid-source MBE system. The Bi, Te_2 and Se_2 fluxes were generated by standard effusion cells installed in the II-VI MBE chamber. The structure and thickness of the films were monitored *in situ* by reflection high-energy electron diffraction (RHEED). The

[a)]Author to whom correspondence should be addressed; electronic mail: xliu2@nd.edu

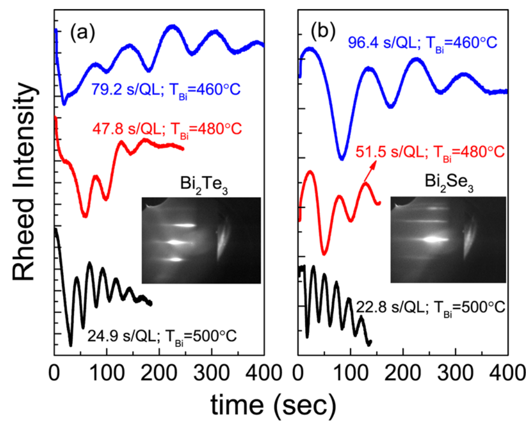

Fig. 1. (Color online) RHEED intensity of the specular point vs growth time under different Bi cell temperatures: (a) Bi_2Te_3 and (b) Bi_2Se_3. Inset: RHEED patterns observed for $[1\bar{1}0]$ direction of the GaAs (001) substrate during MBE growth of: (a) Bi_2Te_3 and (b) Bi_2Se_3.

growth sequence was as follows. First, an epi-ready GaAs (001) substrate was heated to 600 °C for deoxidation in the III-V MBE chamber. This was followed by deposition of a 100 nm GaAs buffer layer. This modified substrate was then transferred to the II-VI MBE chamber through an ultra-high vacuum connection. The growth of the TI film is initiated by deposition of a series of monolayers of Te-Bi-Te-Bi-Te or Se-Bi-Se-Bi-Se—a quintuple layer (QL)—in atomic layer epitaxy (ALE) fashion at room temperature. The substrate was gradually heated to 300 °C, and a streaky RHEED unreconstructed pattern then appeared (see insets of Fig. 1). The MBE growth of Bi_2Te_3, Bi_2Se_3, or their alloys was then performed under Te_2 or Se_2 rich conditions with $T_{substrate} = 300\,°C$. The RHEED patterns shown in insets of Fig. 1 were maintained throughout the entire growth process. It is important to note that the RHEED pattern showed recurrences six times during each rotation of the substrate, which confirms the *c*-axis growth of the TI films, with the *a*-axis lying along either the [110] or the $[1\bar{1}0]$ direction of the GaAs (001) substrate.

At the beginning of growth, RHEED oscillations of the specular spot were observed, with each oscillation corresponding to the growth of one QL. Figure 1 shows RHEED oscillations observed with different temperatures of the Bi cell. As the Bi temperature was increased, the period of the oscillations decreased, indicating that the growth rate was directly controlled by the Bi flux, and that the growth of the TI films proceeded in a QL-by-QL mode. The TI samples grown in this manner were then characterized *ex situ* by atomic force microscopy (AFM), high resolution x-ray diffraction (XRD), Raman spectroscopy and mapping, and transmission electron microscopy (TEM).

III. RESULTS AND DISCUSSION

Figure 2 shows AFM images of Bi_2Te_3 and Bi_2Se_3 films deposited at a growth rate of 2 nm/min, and at the Te_2/Bi beam equivalent pressure (BEP) ratio of ten and Se_2/Bi ratio of 20, respectively. The thicknesses of the Bi_2Te_3 and Bi_2Se_3 layers shown in Figs. 2(a) and 2(b) are 210 and 215

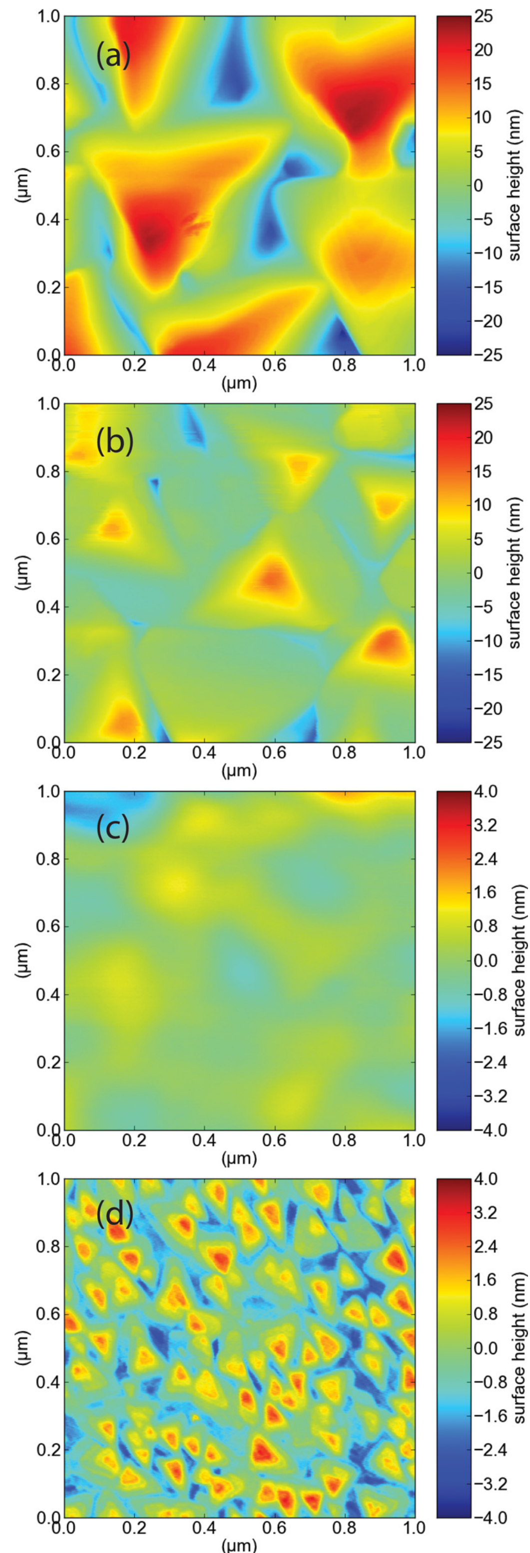

Fig. 2. (Color online) AFM images of Bi_2Te_3 and Bi_2Se_3 samples grown with the Te_2/Bi BEP ratio of ten and Se_2/Bi BEP ratio of 20, respectively. (a) 210-nm-thick Bi_2Te_3; (b) 215-nm-thick Bi_2Se_3; (c) 15-nm-thick Bi_2Te_3; (d) 15-nm-thick Bi_2Se_3.

nm, respectively. The thicknesses of the films shown in Figs. 2(c) and 2(d) are 15 nm. The images show many hills of triangular shape aligned along specific orientations. Our results agree with earlier reports on Bi_2Te_3,[16] and Bi_2Se_3 films,[12]

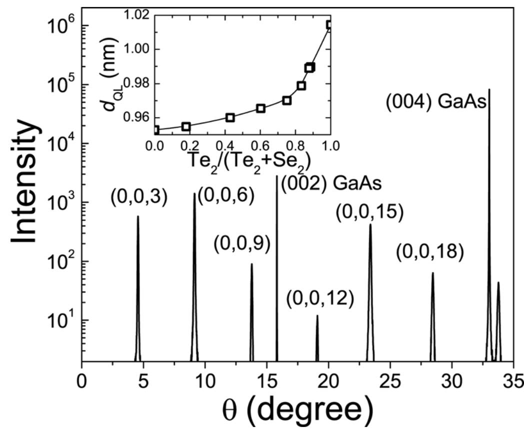

Fig. 3. X-ray diffraction data obtained for a 220-nm-thick $Bi_2(TeSe)_3$ film grown on a GaAs (001) substrate. The (003) family of reflections are labeled, together with (002) and (004) reflections from the GaAs (001) substrate. Inset: QL thicknesses d_{QL} calculated from XRD data for a series of $Bi_2(TeSe)_3$ films plotted as a function of $Te_2/(Te_2+Se_2)$ BEP ratio. The curve is a guide for the eye.

suggesting that the growth of TI films takes place by a step-flow growth mode, with strongly anisotropic Bi adatom diffusion. In addition, as shown in Fig. 2(d), for a 15 nm thick Bi_2Se_3 layer, many small triangular terraces are clearly observed, indicating islandlike growth for very thin films,[13] and suggesting that the mobility of Bi adatoms is much slower on the Bi_2Se_3 surface than on Bi_2Te_3 due to different chemical bond strengths of Bi-Te and Bi-Se. However, as growth proceeds, the surface morphology of Bi_2Se_3 eventually becomes similar to Bi_2Te_3. It is already known that the surface morphology of TI films is dramatically affected by the group-VI/Bi BEP ratio and the growth rate.[16] In fact, in the case of Bi_2Se_3, as we decreased the Bi flux, the surface of thin Bi_2Se_3 layers became much smoother and Bi_2Te_3-like.

The high crystalline quality of the TI films was confirmed by high resolution XRD measurements on a series of $Bi_2(TeSe)_3$ alloy films grown on GaAs (100) substrates with various $Te_2/(Te_2+Se_2)$ BEP ratios. The ternary films were grown in a Te-rich regime by varying Se_2 flux, with a constant of Te_2/Bi BEP of around ten. Representative XRD spectra taken on a 220-nm-thick $Bi_2(TeSe)_3$ alloy film shown in Fig. 3 reveals many reflections from only {003}-type lattice planes, which is indicative of highly directed *c*-axis growth of the TI films.[17] X-ray rocking curves yielded a full-width-at-half maximum of $0.2° - 0.5°$. The QL thicknesses d_{QL} were calculated from the XRD data. As shown in the inset of Fig. 3, the film composition of $Bi_2(TeSe)_3$ based on d_{QL} does not linearly depends on the $Te_2/(Te_2+Se_2)$ BEP ratio, which suggests that Bi favors bonding with Se rather than with Te. This result agrees with our AFM measurements.

Raman spectroscopy and mapping of the TI films was also performed using a 532 nm laser for excitation (at power ~0.8 mW). The results show two characteristic peaks for Bi_2Te_3 [at ~102 cm^{-1} ($E^2{}_g$) and 134 cm^{-1} ($A^2{}_{1g}$)], and three peaks for Bi_2Se_3 [at ~71 cm^{-1} ($A^1{}_{1g}$), 131 cm^{-1} ($E^2{}_g$) and 174 cm^{-1} ($A^2{}_{1g}$)].[17] These peaks are consistent with the lattice vibration modes reported earlier for corresponding bulk materials.[18] In Fig. 4, representative Raman maps (showing position differences of the Raman peak $E^2{}_g$) are plotted for Bi_2Te_3 [Fig. 4(a)] and Bi_2Se_3 [Fig. 4(b)]. These Raman maps show that the position differences of the Raman peaks are less than ~1 cm^{-1} within a scan area of 15 $\mu m \times 15$ μm, indicating a high uniformity of the films.

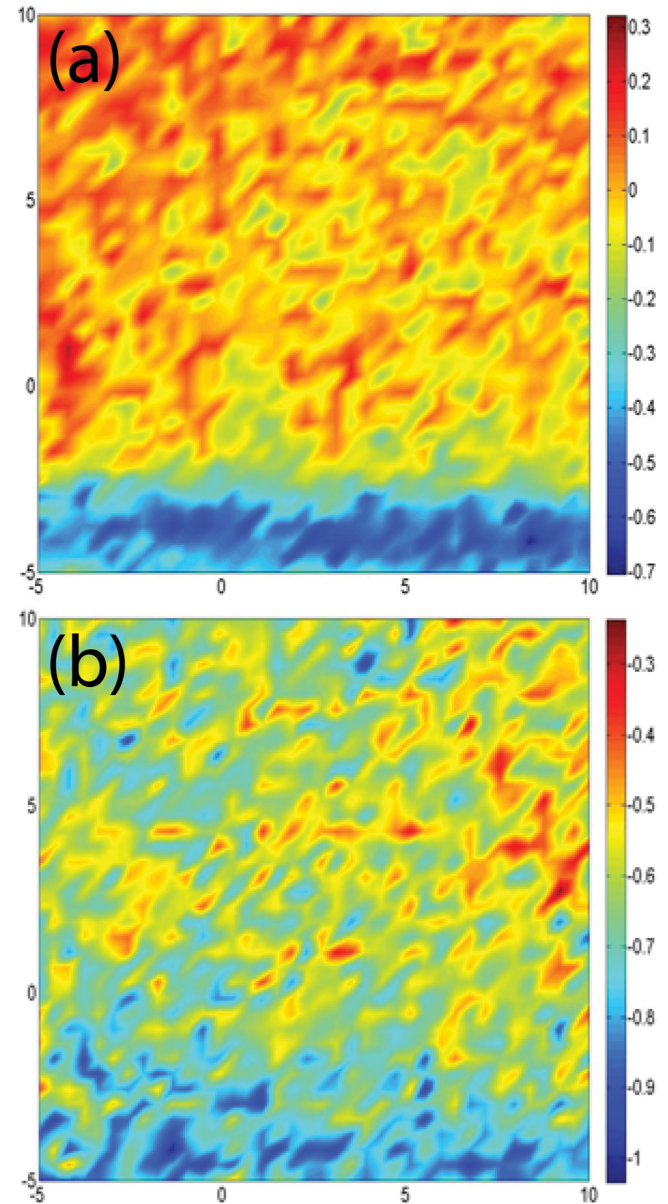

Fig. 4. (Color online) Representative Raman maps (the position differences of the Raman peak $E^2{}_g$) measured within a scan area of 15 $\mu m \times 15$ μm for (a) 136 nm thick Bi_2Te_3 and (b) 150 nm thick Bi_2Se_3. The unit for the scale bars is cm^{-1}.

The microstructure of the films was determined using cross-section transmission electron microscopy (XTEM). Samples were prepared for TEM examination using standard mechanical polishing and argon-ion-milling, with the sample held at liquid-nitrogen temperature during the latter process in order to avoid unintentional ion-milling artifacts. In Fig. 5, XTEM images of Bi_2Te_3 and Bi_2Se_3 layers grown on GaAs (100) buffers show the lattice structure of both the TI

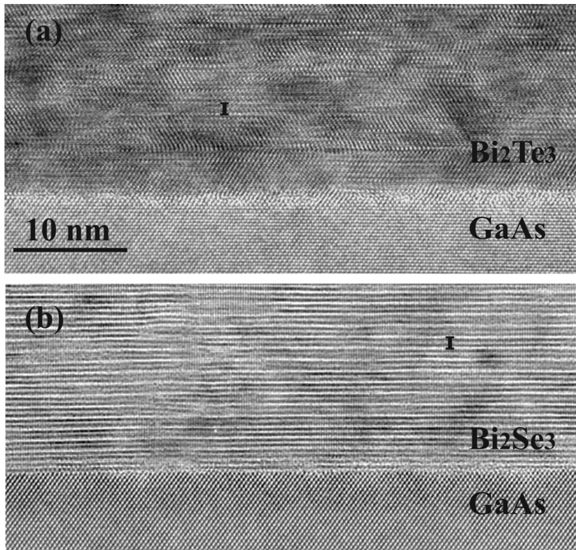

FIG. 5. High-resolution transmission electron microscopy images showing cross sections of topological insulator (a) Bi_2Te_3 and (b) Bi_2Se_3 grown by MBE on a GaAs (001) substrate. The distances between QLs (~1 nm) are shown as "I."

films and the GaAs substrate at their interfaces. Clean interfaces without any amorphous phases are observed, as reported for films grown on GaAs (111) substrates.[13] The highly parallel QLs—Te(Se)-Bi-Te(Se)-Bi-Te(Se)—are visible in both Bi_2Te_3 and Bi_2Se_3 films, marked by the symbol "I" in the figure. Figure 5 suggests that the highly parallel QLs in Bi_2Se_3 film extend over a significantly longer range than those in Bi_2Te_3 films, indicating a particularly strong internal self-correction process in Bi_2Se_3 films that is occurring as the growth proceeds.[17] In addition, despite the symmetry mismatch between the hexagonal lattices of the TI films and the four-fold cubic symmetry of the GaAs (001) surface, the TEM images show that the TI films are highly uniform, and that their crystallinity is comparable to that of films grown on substrates with hexagonal surface structure.

Earlier studies of MBE growth of Bi_2Te_3 on cubic Si (001) substrates[16] appeared to suggest that a hexagonal structure of the substrate surface was essential for epitaxial growth of Bi_2Te_3 film to succeed. In contrast, our work shows that high quality Bi_2Te_3, Bi_2Se_3 and their alloys can form on GaAs (001) substrates with well-defined crystal orientations. This result suggests that the problems encountered in the MBE growth of Bi_2Te_3 films on Si (001) substrates could be caused by the reactivity of Te with Si,[19] rather than being a result of mismatched symmetries at the substrate-TI interface. Our discovery shows that self-correction process during growth of these layered honeycomb materials may play an important role in overcoming differences between crystal arrangements at interfaces during epitaxy.

IV. SUMMARY

In summary, even though there is a mismatch between the hexagonal lattices of Bi_2Te_3 and Bi_2Se_3 TI films and the cubic symmetry of the GaAs (001) surface, we have successfully grown high quality epitaxial films of Bi_2Te_3, Bi_2Se_3 and their alloys on GaAs (001) substrates. The films are highly uniform and the crystallinity is comparable to that of films grown on substrates with hexagonal surface structure. We observed a step flow mode of growth, with strongly anisotropic Bi adatom diffusion, the same as reported previously for TI films. Future studies of TI films grown on GaAs (001) substrates should contribute towards a better knowledge of the MBE growth of TI layered structures; at the same time opening up an opportunity for future spin-based devices that combine topological insulators with ferromagnetic semiconductors.

ACKNOWLEDGMENTS

This work was supported by NSF Grant No. DMR10-05851 (ND); NSF Grant No. ECCS10-02114 and an AFOSR Grant No. FA9550-10-1-0129 (ASU); and DARPA MESO program (Purdue). The authors acknowledge use of facilities in the John M. Cowley Center for High Resolution Electron Microscopy at Arizona State University.

[1]M. Konig, S. Wiedmann, C. Brune, A. Roth, H. Buhmann, L. W. Molenkamp, X. L. Qi, and S. C. Zhang, Science **318**, 766 (2007).
[2]X. L. Qi and S. C. Zhang, Phys. Today **63**, 33 (2010).
[3]M. Z. Hasan and C. L. Kane, Rev. Mod. Phys. **82**, 3045 (2010).
[4]D. Hsieh, D. Qian, L. Wray, Y. Xia, Y. S. Hor, R. J. Cava, and M. Z. Hasan, Nature **452**, 970 (2008).
[5]Y. Xia, L. Wray, D. Qian, D. Hsieh, A. Pal, H. Lin, A. Bansil, D. Grauer, Y. Hor, R. Cava, and M. Hasan, Nat. Phys. **5**, 398 (2009).
[6]Y. L. Chen, J. G. Analytis, J.-H. Chu, Z. K. Liu, S.-K. Mo, X. L. Qi, H. J. Zhang, D. H. Lu, X. Dai, Z. Fang, S. C. Zhang, I. R. Fisher, Z. Hussain, and Z.-X. Shen, Science **325**, 178 (2009).
[7]D. Hsieh, Y. Xia, D. Qian, L. Wray, F. Meier, J. H. Dil, J. Osterwalder, L. Patthey, A. V. Fedorov, H. Lin, A. Bansil, D. Grauer, Y. S. Hor, R. J. Cava, and M. Z. Hasan, Phys. Rev. Lett. **103**, 146401 (2009).
[8]S.-C. Zhang, Physics **1**, 6 (2008).
[9]X. Chen, X.-C. Ma, K. He, J.-F. Jia, and Q.-K. Xue, Adv. Mater. **23**, 1162 (2011).
[10]G. Zhang, H. Qin, J. Teng, J. Guo, Q. Guo, X. Dai, Z. Fang, and K. Wu, Appl. Phys. Lett. **95**, 053114 (2009).
[11]M. Liu, C.-Z. Chang, Z. Zhang, Y. Zhang, W. Ruan, K. He, L. li Wang, X. Chen, J.-F. Jia, S.-C. Zhang, Q.-K. Xue, X. Ma, and Y. Wang, Phys. Rev. B **83**, 165440 (2011).
[12]G. H. Zhang, H. J. Qin, J. Chen, X. Y. He, L. Lu, Y. Q. Li, and K. H. Wu, Adv. Funct. Mater. **21**, 2351 (2011).
[13]A. Richardella, D. M. Zhang, J. S. Lee, A. Koser, D. W. Rench, A. L. Yeats, B. B. Buckley, D. D. Awschalom, and N. Samarth, Appl. Phys. Lett. **97**, 262104 (2010).
[14]J. Sadowski, R. Mathieu, P. Svedlindh, J. Z. Domagała, J. Bak-Misiuk, K. Świątek, M. Karlsteen, J. Kanski, L. Ilver, H. Åsklund, and U. Södervall, Appl. Phys. Lett. **78**, 3271 (2001).
[15]J. J. Krebs, B. T. Jonker, and G. A. Prinz, J. Appl. Phys. **61**, 2596 (1987).
[16]J. Krumwain, G. Mussler, S. Borisova, T. Stoica, L. Plucinski, C. M. Schneider, and D. Grützmacher, J. Cryst. Growth **324**, 115 (2011).
[17]X. Liu, D. J. Smith, J. Fan, Y.-H. Zhang, H. Cao, Y. P. Chen, J. Leiner, B. J. Kirby, M. Dobrowolska, and J. K. Furdyna, Appl. Phys. Lett. **99**, 171903 (2011).
[18]W. Richter, H. Kohler, and C. R. Becker, Phys. Status Solidi B **84**, 619 (1977).
[19]P. K. Shufflebotham, H. C. Card, K. C. Kao, and A. Thanailakis, J. Appl. Phys. **60**, 2036 (1986).